Stimulation of Insulin Signaling Reverses Inflammation-Induced Cone Death in Retinal Detachment

Jean-Baptiste CONART (jbconart@hotmail.com)
Universite de Lorraine https://orcid.org/0000-0001-6348-6165
Guillaume Blot
Institut de la vision
Sébastien Augustin
Institut de la vision
Christophe Roubeix
Institut de la vision
Fanny Beguier
Institut de la vision
Hugo Charles-Messance
Institut de la vision
Sara Touhami
Institut de la vision
José-Alain Sahel
Institut de la vision
Jean-Paul Berrod
Universite de Lorraine
Xavier Guillonneau
Institut de la vision
Cécile Delarasse
Institut de la vision
Florian Sennlaub
Institut de la vision

Research

Keywords: retinal detachment, cone degeneration, inflammation, mononuclear phagocytes, insulin signaling

Posted Date: May 29th, 2020

DOI: https://doi.org/10.21203/rs.3.rs-30991/v1

Version of Record: A version of this preprint was published on November 26th, 2020. See the published version at https://doi.org/10.1186/s12974-020-02039-1.

Abstract

Background Rhegmatogenous retinal detachment (RD) involving the macula is a major cause of visual impairment despite high surgical success rate, mainly because of cone death. We and others have shown that cone loss occurs secondary to chronic inflammation in many retinal diseases, including age-related macular degeneration and retinitis pigmentosa. We here investigated the yet unknown mechanisms of inflammation-induced cone death in RD.

Methods Vitreous samples from patients with RD and from control patients with macular hole were analyzed to characterize the inflammatory response to RD. A mouse model of RD and retinal explants culture were then used to explore the mechanisms leading to cone death.

Results Analysis of vitreous samples shows that RD induces a marked inflammatory response with increased cytokine and chemokine expression in humans, which is closely mimicked by experimental murine RD. In this model, we demonstrate that myeloid cells and T-lymphocytes directly contribute to cone loss, as the inhibition of their accumulation by Thrombospondin 1 increased cone survival. We show that cones are highly dependent on glucose and insulin signaling for survival *in vitro* and that insulin, and the insulin sensitizers rosiglitazone and metformin, prevent RD-induced cone loss *in vivo*, despite the persistence of inflammation.

Conclusion Our results describe a new mechanism by which inflammation, likely through a combination of competition for glucose and the inhibition of insulin signaling, promotes cone death in RD. Therapeutic inhibition of inflammation and stimulation of insulin signaling might prevent RD-associated cone death until the RD can be surgically repaired and improve visual outcome after RD.

Trial registration: ClinicalTrials.gov Identifier NCT03318588

Background

Rhegmatogenous retinal detachment (RD) is a sight-threatening condition with an annual incidence of 10.5 per 100,000 people [1]. Advances in surgical techniques over recent decades have greatly improved the anatomical results with a primary success rate currently up to 80% [2]. However, despite a successful retinal reattachment, visual recovery may still be disappointing, especially in cases involving the cone-rich macula [3] and this loss of vision is primarily due to photoreceptor cell death [4, 5]. Several pathogenic mechanisms have been identified but accumulating evidence suggests that inflammation plays a key role in the pathogenesis of RD-induced rod-photoreceptor cell death. Human studies have thus reported elevated levels of cytokines and chemokines in the vitreous of patients with RD [6–9]. Furthermore, experimental models have demonstrated that cytokines from infiltrating mononuclear phagocytes (MP) induce the death of rods following retinal detachment [10–13].

Although cones represent only 5% of all photoreceptor cells in humans, they are responsible for daylight, high-acuity and color vision. In retinal detachment, cone density decreases despite successful surgery

and there is a strong correlation between post-operative cone density and visual acuity [14]. It is therefore important to identify the yet unknown mechanisms of detachment-associated cone death to establish therapeutic targets for preventing visual impairment.

Cones are highly metabolically active cells which particularly depend on glucose for function and long-term survival [15, 16]. Contrary to muscle and fat (in which glucose absorption is mediated by the insulin-dependent Glucose transporter 4 (GLUT4)), glucose uptake in adult neurons depends mainly on the insulin-independent GLUT3 [17]. Interestingly, cone glucose uptake relies on GLUT1, which is regulated by the Rod-derived cone viability factor (RdCVF) [15, 16], and the Insulin/mTOR pathway [18, 19]. Indeed, cones have their own endogenous insulin receptor signaling pathway including the phosphoinositide 3-kinase (PI3K) and m-TOR and cone-specific deletion of PI3K (p85) is sufficient to induce age-related cone degeneration [20, 21]. In retinitis pigmentosa, where RdCVF levels are extinguished due to the primary loss of rods, systemic administration of insulin improved glucose uptake in cones and delayed their death, despite the absence of RdCVF [18, 19]. Together these studies reveal the crucial role of insulin signaling in cone viability.

Inflammatory cells, are also very reliant on glucose for metabolic activity, in particular when activated [22]. Their glucose uptake is mainly insulin-independent and mediated by GLUT1 and GLUT3 [17]. On the other hand, these leukocytes can produce cytokines such as IL-1ß, IL-6, and IFN-γ, which inhibit insulin signaling in adjacent stromal cells, an important mechanism of type 2 diabetes [23]. In RD, it is not clear whether and to what degree infiltrating inflammatory cells disturbe insulin signaling and cone glucose availability.

We here demonstrate, using human vitreous samples and a mouse model of RD, that RD causes a severe inflammatory response characterized by increased cytokine expression. In experimental RD, we demonstrate that the recruitment of myeloid cells and T-lymphocytes directly contribute to cone loss in RD. We show that cones are highly dependent on insulin signaling for survival *in vitro* and that insulin and the insulin sensitizers rosiglitazone and metformin prevent RD-induced cone loss *in vivo*, despite the persistence of subretinal MP accumulation. Taken together, our results suggest that infiltrating MPs contribute to cone death by reducing the availability of glucose and inhibiting insulin signaling. Improving insulin signaling in cones might represent a therapeutic target for delaying RD-associated cone degeneration and subsequent vision loss.

Methods

Patients

We conducted a nonrandomized clinical study at Nancy University Hospital from November 2017 to August 2018. Forty-one patients with primary RD requiring vitrectomy and 33 control patients undergoing vitrectomy for vitreomacular traction (VMT) or macular hole (MH) were included in this study.

Exclusion criteria were any history of vitreoretinal surgery on the eye studied, diabetic retinopathy or uveitis.

All patients underwent a detailed ophthalmologic examination before surgery, including best-corrected visual acuity measured with projected-light Snellen charts, axial length measurement using IOLMaster (Carl Zeiss Meditec, Dublin, CA), biomicroscopy with anterior segment evaluation, fundus and careful peripheral retina examination. For the RD group, an Amsler-Dubois scheme was systematically established for each patient, specifying the extent of the RD, number, type and location of retinal breaks, existence of vitreous hemorrhage and preoperative proliferative vitreoretinopathy (PVR) grading according to Machemer et al [24].

All patients underwent a three-port 23- or 25-gauge pars plana vitrectomy. At the beginning of vitrectomy, air perfusion was set to open and undiluted vitreous fluid samples (1 mL) were collected from each eye with 3 mL syringe. Samples were sent to the Biological Resource Center (Centre de Ressources biologiques, Nancy, France) within 30 min, cooled on ice and transferred into microfuge tubes. Each sample was centrifuged at 10000 g for 5 min and the supernatant was then collected and frozen at -80 °C before analysis.

Multiplex bead immunoassay

Inflammatory cytokine concentrations were measured using Bio-Plex Pro™ Human Cytokine 27-plex Assay (Bio-Rad Laboratories, Marnes-la-Coquette, France). Briefly, vitreous samples were thawed and diluted twofold through the use of the dilution solution provided by the Bio-Plex beads array kit. Cytokine levels were measured in duplicate with 50 µL of diluted supernatant in accordance with the manufacturer's instructions. The following 27 cytokines and chemokines were targeted: IL-1ß, IL-1 receptor antagonist (IL-1ra), IL-2, IL-4, IL-5, IL-6, IL-7, IL-8 [chemokine C-X-C motif ligand (CXCL)8], IL-9, IL-10, IL-12, IL-13, IL-15, IL-17, eotaxin [chemokine C-C motif ligand (CCL)11], basic fibroblast growth factor (b-FGF), granulocyte colony-stimulating factor (G-CSF), granulocyte/macrophage colony-stimulating factor (GMCSF), interferon (IFN)-γ, interferon-inducible 10-kDa protein [IP-10 (CXCL10)], MCP-1 (CCL2), macrophage inflammatory protein-1 [MIP-1α (CCL3)], MIP-1ß (CCL4), platelet-derived growth factor (PDGF), regulated upon activation, normal T cell expressed and secreted [RANTES (CCL5)], tumor necrosis factor (TNF)-α, and VEGF (vascular endothelial growth factor).

Mouse model of RD

Wild-type (C57BL/6J) mice were purchased from Janvier Labs at the age of 8 weeks. Mice were housed in the animal facility under specific pathogen-free condition, in a 12 h/12 h light/dark (100–500 lux) cycle with water and normal diet food available *ad libitum*. All experimental protocols and procedures were approved by the local animal care ethics committee (N°APAFIS#5201-20160427103344).

RD was induced with a previously described method [11–13]. Briefly, mice were anesthetized with an intraperitoneal injection of xylazine hydrochloride (10 mg/kg) and ketamine hydrochloride (100 mg/kg) and pupils were dilated with topical phenylephrine (5%) and tropicamide (0.5%). A 30-gauge needle was

first used to create two sclerotomies 1.5 mm posterior to the limbus. A glass needle (with a 80-gauge manually beveled tip) connected to a Hamilton syringe filled with diluted sodium hyaluronate (Healon GV®, Alcon) was then introduced into the vitreous cavity through one of the sclerotomy. The

tip of the needle was finally inserted into the subretinal space through a peripheral retinotomy and 4 µl of diluted sodium hyaluronate containing or not recombinant human TSP-1 (thrombospondin-1) (100 µg/ml, Biotechne), human insulin (2 IU/ml, Umuline NPH), recombinant IGF-1 (insulin growth factor-1) (200 ng/ml, Biotechne) or metformin (50 mg/ml, Merck Millipore), was gently injected, detaching approximately two-third of the retina from the underlying RPE.

For treatment with rosiglitazone, mice received intraperitoneal injections of 10 mg/kg rosiglitazone or vehicle (5% DMSO) 3 days before and 4 to 7 days after RD induction.

Eyes with subretinal hemorrhage were excluded from analysis. Mice were sacrified from 1 to 10 days following RD, according to the experiment

Retinal explants culture

C57BL/6J retina were prepared and placed on polycarbonate filters floating on Dulbecco's modified Eagle's medium (DMEM, Thermo Fisher Scientific) with the photoreceptors facing down. For the experiment, retinal explants were cultured in high glucose (25 mM) DMEM alone or supplemented with human insulin (Umuline NPH), human insulin and insulin receptor inhibitor (Hydroxy-2-naphthalenylmethylphosphonic acid (HNMPA), Abcam) or vehicle (DMSO (dimethyl sulfoxide)) at 37 °C. As insulin has been demonstrated to be quite unstable in media containing cysteine [25], and porcine/human insulin (identical except one amino acid at the C-terminus of the beta chain) is significantly less effective in rodents [26], we used supraphysiological doses of insulin (5 mIU/ml) in our model. For this reason, HNMPA was used at a concentration 10-fold higher than the IC50 (1 mM). Each culture medium was renewed every 36 hours and after 5 days, the retinal explants were carefully removed. Immunohistochemistry and cones quantification were then performed as described for retina below.

Isolation of retinal immune cells and flow cytometry analyses

Retinas were dissected out and homogenized in 500 µL of PBS (phosphate buffered saline) with liberase TL at 0.8 wunsch/mL (Sigma-Aldrich) for 30 min at 37 °C and 5% CO_2. The retinal homogenate was washed with PBS and the pellet containing the immune cells was re-suspended in 100 µL PBS containing 1 µL of Viobility 405/520 Fixable Dye (Miltenyi). Cells were washed and labelled with 50 µL of primary antibodies mix: anti-CD45-VioBlue (REA737), anti-MHCII-FITC (REA813), anti-CD11b-PE (REA592), anti-Ly-6C-PE-Vio770 (REA796), anti-CD3-APC (REA641) and anti-Ly-6 g-APC-Vio770 (REA526) (Miltenyi). After labeling, cells were fixed in 4% paraformaldehyde. For compensation settings, single-stained cellular controls with corresponding antibodies were used. Fluorescence intensities were measured using a MACSQuant analyzer (Miltenyi) and data were analyzed using the FlowJo Software.

Immunohistochemistry of retinal flatmounts

Eyes were enucleated, fixed in 4% paraformaldehyde for 1 hour at room temperature and sectioned at the limbus; the cornea and lens were discarded. The retinas were peeled from the RPE/choroid/sclera and incubated overnight at 4 °C in PBS-1% triton with the following primary antibodies: peanut agglutinin (PNA) Alexa fluor® 594 (Thermo Fisher Scientific; 1/100), rabbit polyclonal anti-human cone arrestin (CAR) antibody (LUMIF-hCAR; 1:10000) and goat polyclonal anti-IBA1 (ionized calcium-binding adaptater molecule-1) (Abcam; 1:100). After few washes, the retinas were incubated for 2 hours at room temperature with appropriate Alexa Fluor® conjugated secondary antibodies (Thermo Fisher Scientific; 1:500) in PBS-1% triton and nuclei were counterstained with Hoechst (1:1000, Sigma Aldrich). The retinas were flatmounted and viewed with a fluorescence microscope (DM5500, Leica). Images centered on the area with the lowest number of PNA + cone arrestin + cells were captured with a confocal laser-scanning microscope (FV1000, Olympus) using a 40X lens. Each cell population was manually counted in a masked fashion. IBA-1 + cells were quantified on flatmounts on the outer segment side of the detached retina while PNA + cone arrestin + cells were counted on confocal microscopy Z-stacks using ImageJ software.

Reverse transcription and real-time quantitative polymerase chain reaction

Total RNA was extracted from mouse retina with the Nucleospin RNAII extraction kit according to the manufacturer's protocol (Macherey Nagel). Single-stranded cDNA was synthetized from total mRNA (pretreated with DNase) using oligo-dT as primer and superscript II reverse transcriptase (Thermo Fisher Scientific). Subsequent RT-PCR was performed using cDNA, PowerSYBR Green PCR Master Mix (Applied Biosystems) and primers (IDT technology) available upon request. qPCR was performed using StepOne Plus real-time PCR systems (Applied Biosystems) with the following profile: 45 cycles of 15 s at 95 °C, 45 s at 60 °C. Results were normalized using house-keeping gene RPS26.

Statistical analysis

Graph Pad Prism 7 (GraphPad Software) was used for data analysis and graphic representation. All values are reported as mean ± SEM. Statistical analyses were performed by one-way Anova analysis of variance, Student *t*-test or Mann-Whitney *U* test for comparison among means depending on the experimental design. The *p* values are indicated in the figure legends.

Results

RD causes a marked inflammatory response with increased cytokine and chemokine expression in both human and experimental models

To characterize the inflammatory response to RD, we first analyzed the expression profile of cytokines in vitreous samples from 41 patients with RD and from 34 control patients with macular hole. The mean

extent of detachment in the RD group was 2.1 ± 0.8 quadrants with a macular involvement in 34.1% of cases and some degree of retinal wrinkling and folding (grade B or C proliferative vitreoretinopathy) in 36.6% of cases. The mean duration of symptoms before surgery was 7.7 ± 7.3 days with a median of 4.5 days [1–30]. Using a Human Cytokine 27-plex Assay we showed that the cytokines IL-1ra, IL-6, IL-7, IL-8, IFN-γ (Fig. 1A), the chemokines CCL2, CCL3, CCL4, CXCL10 and CCL11 (Fig. 1B) and the growth factor G-CSF (Fig. 1C) were significantly increased in the vitreous from RD patients. In contrast, the levels of IL-10, IL-13 and VEGF were not statistically different between the two groups (Fig. 1A-C). The remaining cytokines, such as IL-4, and IL-17 of the assay were not detectable.

We next evaluated the expression of the cytokines by RT-qPCR of mouse retinal control tissues and retinas harvested after four days of experimental RD. This time point was chosen for analysis as it was similar to the median duration of symptoms in our clinical study and because photoreceptor cell death peaks at around three days after RD in both experimental models and human samples [4, 27–29]. The transcription levels of nine out of eleven mediators found to be elevated in human vitreous from RD patients (except for *Ccl11* and *Il-8* that does not exist in mice*)* were significantly upregulated in detached mouse retinas compared to controls (Fig. 1D-F).

In summary, our findings confirm that RD induces a marked inflammatory response in human patients, which is closely mimicked by experimental murine retinal detachment. The cytokine profil is suggestive of an infiltration of mainly myeloid cells, but the increased levels of IFN-γ might be suggestive of T helper type 1 (Th1) cells recruitment.

RD-associated leukocyte infiltration is associated with cone loss

In the healthy retina, microglial cells (MCs) populate the inner retina, but the photoreceptor cell layer and subretinal space are devoid of any immune cells [30]. In RD, MPs have been shown to accumulate in the detached area and are highly associated with TUNEL-positive nuclei in the inner aspects of the outer nuclear layer (ONL), where rod nuclei are located [10, 12, 13]. Using flow cytometry and a gating strategy (Fig. 2A) adapted from O'Koren et al. [31], we here analyzed the leukocyte population in healthy and detached (day 1, day 3, day 7) mouse retinas. In healthy retinas, we only detected MCs ($CD11b^{+}CD45^{low}$) that steadily increased to quadruple their numbers at the end of the observation period (Fig. 2B). The myeloid cell population ($CD11b^{+}CD45^{high}$) sharply increased after RD, peaking at 24 h and remained strongly elevated throughout (Fig. 2B). Interestingly, we also found a sizeable population of T-cells ($CD45^{+}CD3^{+}$) that infiltrated the retina at day 3 and remained elevated, although to a lesser extent, at day 7 (Fig. 2B). A more detailed analysis of the myeloid population reveals a rapid, but short-lived recruitment of neutrophils ($CD11b^{+}CD45^{high}Ly6G^{+}$) and monocytes ($CD11b^{+}CD45^{high}Ly6G^{neg}Ly6C^{high}$) at day 1 (Fig. 2C). The number of macrophages ($CD11b^{+}CD45^{high}Ly6G^{neg}Ly6C^{low}$) mainly increased at day 3 and stayed elevated, likely reflecting the differentiation of monocytes (Mos) into macrophages (Fig. 2C). Together, these results demonstrate that RD induces the infiltration of T-cells, monocyte derived-

macrophages (Mφs) and accumulation of MCs, and that MPs, MCs and Mφs, represent the main accumulating immune cells.

Next, we quantified the presence of MPs (MCs and Mφs) and the cone population on IBA-1 (MP marker)-, peanut agglutinin (PNA cone outer segment marker)-, cone arrestin (CAR, cone marker) triple-stained retinal flat-mounts (Fig. 2D). Confocal microscopy confirmed that subretinal MPs are not observed in normal mice and highlight the elongated shape of the cone outer segments (Fig. 2D). Interestingly, despite the peak of infiltrating myeloid cells measured in the whole retina at day 1, IBA-1$^+$MPs only accumulated in the subretinal space by day 3 and continued to rise to reach a plateau at day 7 (Fig. 2E). Although cone outer segments seemed shortened at day 1 (Fig. 2D), their number only decreased significantly in the following days and was reduced by approximately 50% at day 7 (Fig. 2D, F and G) mirroring the subretinal MPs accumulation.

Taken together, our results demonstrate that RD leads to a rapid infiltration of myeloid cells, followed by T-cells and a protracted increase of the numbers of MCs and Mφs that started accumulating in the subretinal space by day 3. We also showed that this accumulation was strongly associated with cone death.

TSP-1 inhibits RD-induced subretinal MPs infiltration and associated cone loss

Thrombospondin-1 (TSP-1) is an extracellular matrix molecule that is produced by a wide variety of cell types, notably the RPE, inflammatory and resident macrophages [30]. We and others have shown that it physiologically prevents age-related subretinal MP accumulation and inhibits excessive subretinal MP infiltration and choroidal neovascularization in the context of age-related macular degeneration [32–34] and controls T-cell response [35]. To further explore the role of infiltrating MPs in RD-associated cone loss, we induced RD with diluted sodium hyaluronate that contained or not recombinant TSP-1 (100 µg/ml). Using flow cytometry and the same gating strategy as in Fig. 2 (Fig. 3A), we found that recombinant TSP-1 significantly reduced the number of T-cells, Mos, and Mφs but had no effect on the MC population (Fig. 3B). Accordingly, RT-qPCR analysis showed that recombinant TSP-1 significantly reduced the transcription levels of *Il-6*, *Ifn-γ, Ccl2*, *Ccl3* and *Ccl4* (Fig. 3C). Quantification of IBA-1$^+$MPs and PNA$^+$CAR$^+$cones on triple-stained retinal flat-mounts at day 7 (Fig. 3D) showed that recombinant TSP-1 also significantly decreased subretinal MP accumulation (Fig. 3E) and increased cone survival in detached retinas compared with PBS controls (Fig. 3F and 3G).

Together, these findings show that the pharmacologically induced reduction of the population of infiltrating MPs and T-cells and cytokines expression significantly protects against RD-induced cone loss, suggesting that infiltrating T-cells, Mos, and Mφs directly contribute to cone loss in RD.

Insulin is essential for cone survival in vitro **and delays RD-induced cone loss** in vivo

Cones are highly dependent on glucose for metabolic activity and long term survival [15, 16]. It has been shown that insulin signaling pathways play a key role in cone glucose uptake [20, 21] and that activation of these pathways by systemic injection of insulin promotes cone survival in a mouse model of RP [18, 19].

In RD, cone glucose availability could become critical as highly metabolic active immune cells compete for fuel in the photoreceptor cell layer [22]. Additionally, inflammatory cytokines such as IL-6, and IFN-γ might impede with insulin signaling, similar to the mechanism of type 2 diabetes [23].

To investigate whether diminished insulin signaling could contribute to RD-associated cone loss in adult retinas, we first examined the effect of insulin on 5 day retinal explants with or without human insulin and/or the specific insulin receptor inhibitor HNMPA (Fig. 4A). Quantification of PNA^+CAR^+ cones showed that cone survival was significantly increased in the presence of insulin in the medium culture compared to the control condition (Fig. 4A and 4B). The addition of an insulin receptor inhibitor HNMPA that blocks insulin receptor autophosphorylation, but not insulin growth factor 1 (IGF-1) receptor activation [36], resulted in a severe loss of PNA^+CAR^+ cones, not observed with its vehicle (DMSO) (Fig. 4A and 4B). Our results indicate that insulin signaling promotes cone survival in retinal explants confirming previous results in a mouse retinal degeneration model [18, 19].

Next, we induced RD *in vivo* with subretinal injection of diluted sodium hyaluronate containing (or not) human insulin (2 IU/ml). Quantification on immuno-stained retinal flat-mounts at day 7 (Fig. 4C) revealed that insulin treatment did not alter the numbers of subretinal $IBA1^+$ MPs, but very significantly increased the number of PNA^+CAR^+ cones compared to PBS controls (Fig. 4D-F). Comparatively, addition of IGF-1 to the detachment inducing gel (at a concentration 100-fold higher than IGF-1 s ED50, which has been shown to reverse hypoalgesia in diabetic mice [37]) had no effect on the numbers of $IBA1^+$ MPs or PNA^+CAR^+ cones, quantified on day 7 immuno-stained retinas (Fig. 4G-J).

Taken together, our results showed that insulin and insulin receptor signaling were essential for cone survival *ex vivo* of adult retinas and that insulin treatment very significantly inhibited RD-induced cone loss despite the unchanged MPs infiltration *in vivo*. This effect was not due to insulin-induced IGF-1R signaling, which can activate anti-apoptotic IGF-1 receptor signaling [38, 39], as IGF-1 had no comparable effect.

The insulin sensitizer rosiglitazone and metformin prevent RD-induced cone loss

IL-6 and IFN-γ, which we show are increased in RD, can inhibit insulin signaling in type 2 diabetes [23]. This insulin resistance can at least in part be reversed by insulin sensitizers, such as rosaglitazone [40, 41]. To explore whether pharmacological improvement of insulin-signaling could reduce inflammation-induced cone degeneration in RD, we next examined whether rosiglitazone, could prevent cone loss in our mouse model of RD.

Mice received daily intraperitoneal injections of rosiglitazone or vehicle (DMSO 5%) 3 days before and throughout the 7 days of RD. The treatment also did not alter the increased levels of *Il-6* and *Ifn-γ* mRNA levels in whole retinal mRNA and increased *Ccl2* in four day RD samples (Fig. 5A). Quantification of IBA1-, PNA-, CAR triple-stained retinal flatmounts (Fig. 5B) also showed that rosiglitazone had no effect on the number of infiltration of subretinal IBA-1$^+$ MPs at day 7 (Fig. 5C). Despite this lack of an anti-inflammatory effect, quantification of PNA$^+$CAR$^+$ cones, revealed that rosiglitazone significantly protected retinas against cone loss at day 7 (Fig. 5D and E). Interestingly, subretinal injection of metformin, a commonly used insulin sensitizer that also exerts an independent anti-inflammatory effect [42, 43], significantly increased cone survival and decreased subretinal MP accumulation in detached retinas compared with PBS controls (Fig. 5G-J).

In summary, our results show that the well-established insulin sensitizers rosiglitazone and metformin significantly curb cone loss in RD. The fact that we observed increased cone survival under rosiglitazone- and insulin- treatment in the absence of an anti-inflammatory effect strongly suggests that restored insulin signaling was the likely mode of action.

Discussion

Despite successful surgical repair, visual recovery remains incomplete in many eyes that have suffered from macula-off RD, mainly because of photoreceptor cell death [4, 5, 27], in particular cone loss [14]. Although evidence from both human and experimental studies show that inflammation is strongly associated with RD-induced photoreceptor cell death [7, 10–13], little is known about the mechanisms that specifically lead to cone death.

Our analysis of vitreous samples confirms that RD in humans is associated with increased expression of cytokines, chemokines and growth factors [6, 7, 9, 44]. Interestingly, our experimental model revealed a very similar induction in RD in mice, making it therefore well-suited for studying the effect of these mediators on RD-associated cone loss. We confirm previous reports of RD-induced MP accumulation [7, 10, 12, 45–47]. Our flow cytometric analysis showed a more nuanced picture of a rapid infiltration of neutrophils and Mos (day 1), followed by T-lymphocytes (day 3) and a protracted increase of the numbers of MCs and Mφs that were immunohistochemically detected in the subretinal space from day 3 following RD.

RD-induced MP accumulation has previously been shown to be highly associated with TUNEL-positive nuclei in the inner aspects of the ONL, where the rod nuclei are located [10, 12, 13]. We here show that the accumulation of immune cells was strongly associated with the loss of more than 50% of the cones. This loss was demonstrated by the disappearance of PNA$^+$ cells (which might have suggested the loss of cone outer segments only), but also CAR$^+$ cells, a marker that is found throughout the cone cytoplasme, demonstrating the loss of the cells. Recombinant TSP-1 severely reduced the numbers of accumulating infiltrating T-cells, Mos and Mφs, but interestingly not MCs, and very significantly reduced the transcription level of cytokines at day 4, which strongly suggests they were expressed by the leukocytes.

Importantly, TSP-1 treatment also significantly prevented the loss of cones at day 7, suggesting that infiltrating T-cells, Mos, and Mφs directly contribute to cone loss in RD, similarly to previous results regarding rods [10, 12, 13].

Cones are particularly reliant on glucose and insulin signaling for survival [15, 16], evidenced by progressive cone loss in mice with cone-specific deletion of PI3K (p85, indispensible for insulin signaling) [20, 21] and the protective effect of insulin on secondary cone-loss in retinitis pigmentosa [18, 19]. Using insulin and a specific insulin receptor inhibitor on mouse retinal explants, we confirmed that insulin receptor signaling was essential for cone survival *ex vivo*.

During RD the retina is infiltrated by activated leukocytes. Leukocyte activation induces a metabolic switch in the immune cells to aerobic glycolysis, which dramatically increases their glucose consumption and makes them very reliant on surrounding glucose concentrations for survival and function [22]. In RD the infiltrating activated leukocytes therefore likely compete for glucose, which might become critical for cone survival. Upon activation of the leukocytes, GLUT1 (lymphocytes) and GLUT3 (monocytes) are recruited to the plasma membrane mediating the massive glucose uptake [17, 48]. Insulin only plays a minor role in the increased uptake of glucose in inflammatory cells, as it does not influence GLUT translocation to the plasma membrane in neutrophils and T-lymphocytes and only marginally increases glucose consumption in macrophages [48, 49]. Insulin supplementation could therefore redirect glucose uptake preferentially to cones and save cones from starvation. To make matters worse, the inflammatory cytokines, such as IL-6 and IFN-γ, that are secreted by the infiltrating leukocytes, can inhibit insulin signaling, which inhibits insulins trophic effects and further reduces glucose uptake [23]. Inflammation-induced reduced insulin signaling and glucose uptake is increasingly recognized to play an important role in insulin-resistance in the adipose tissue of type 2 diabetes [23], but has also been suggested to play an important role in neuronal death in uveitis, a blinding auto-immune disease of the retina and choroid [50].

To evaluate if glucose could be redirected to cones and trophic signals restored, we treated the experimental animals with insulin or the insulin sensitizer rosiglitazone. Our data demonstrates that insulin supplementation, but also treatment with rosiglitazone, significantly prevented RD-induced cone loss, despite having no effect on the level of inflammation. In contrast, IGF-1 supplementation did not increase cone survival in RD, underlining the specificity of insulin signaling for this effect.

Mechanistically, insulin receptor signaling has been described to increase the GLUT1-dependent glucose uptake via the activation of the mammalian target of rapamycin complex 1 (mTORC1) [18, 19]. In RD, the insulin supplementation might thereby increase glucose-uptake to cones without affecting the insulin-independent glucose uptake by infiltrating leukocyte. This redirection of glucose to the cones could prevent cone starvation in RD. Additionally, insulin and insulin sensitizers might restore the inflammation–induced reduction in insulin receptor signaling and boost the trophic, anti-apoptotic signals via mTORC2 [18, 19]

Conclusion

In summary, our results describe a new mechanism by which inflammation induces cone death in RD. This mechanism might not be specific to RD but could also be involved in other retinal diseases characterized by chronic inflammation and cone loss such as retinitis pigmentosa and AMD [32, 51]. Therapeutic inhibition of inflammation and restoration of insulin signaling and glucose availability to cones might prevent cone death in these diseases. Indeed, our study demonstrates that Metformin, an insulin sensitizer with known anti-inflammatory effects [42, 43], significantly decreased inflammation and increased cone survival. Metformin or similar agents might prevent RD-associated cone death until the RD can be surgically repaired in the future.

Abbreviations

RD
retinal detachment; MP:mononuclear phagocytes; RdCVF:Rod-derived cone viability factor; PI3K:phosphoinositide 3-kinase; VMT:vitreomacular traction; MH:macular hole; PVR:proliferative vitreoretinopathy; IL:interleukin; IL-1ra:IL-1 receptor antagonist; CCL:chemokine C-C motif ligand; CXCL:chemokine C-X-C motif ligand; b-FGF:basic fibroblast growth factor; G-CSF:granulocyte colony-stimulating factor; GMCSF:granulocyte/macrophage colony-stimulating factor; IFN-γ:interferon-γ; MIP:macrophage inflammatory protein-1; PDGF:platelet-derived growth factor; RANTES:normal T cell expressed and secreted; TNF-α:tumor necrosis factor-α; VEGF:vascular endothelial growth factor; TSP-1:thrombospondin-1; IGF-1:insulin growth factor-1; DMEM:Dulbecco's modified Eagle's medium; HNMPA:Hydroxy-2-naphthalenylmethylphosphonic acid; DMSO:dimethyl sulfoxide; PNA:peanut agglutinin; CAR:cone arrestin; IBA-1:ionized calcium-binding adaptater molecule-1; ONL:outer nuclear layer; Th-1 cells:T helper type 1 cells; MCs:microglial cells; Mφs:monocyte derived-macrophages; Mos:monocytes.

Declarations

Ethics approval and consent to participate

This study was approved by the regional Institutional Ethics Committee (Comité de Protection des Personnes CPP17-059/2017-A02195-48) and adhered to the Declaration of Helsinki. This study was also registered in the database of the National Institutes of Health at clinicaltrials.gov (identification number NCT03318588). All patients had complete information about the study and the risks and benefits of the surgical procedure and gave their written consent for participation before surgery.

Consent for publication

Not applicable

Availability of data and materials

All data generated or analyzed during this study are included in this published article. The datasets used and/or analyzed during the current study are also available from the corresponding author on reasonable request.

Competing interests

The authors declare that they have no competing interests.

Funding

This work was supported by grants from INSERM, Unadev/Aviesan M17JRIN005 ANR MACLEAR (ANR-15-CE14-0015-01), LABEX LIFESENSES [ANR-10-LABX-65] supported by the ANR (Investissements d'Avenir programme [ANR-11-IDEX-0004-02]), IHU FOReSIGHT [ANR-18-IAHU-0001] supported by French state funds managed by the Agence Nationale de la Recherche within the Investissements d'Avenir program, Carnot and by Association de Prévoyance Santé de ALLIANZ.

Author's contributions

J-BC designed and performed experiments, analyzed data, and wrote the paper; GB designed and performed experiments, analyzed data; SA, CR, FB, HCM, and ST designed and performed experiments; J-AS and J-PB collected samples and analyzed data; XG and CD performed experiments, analyzed data, and helped write the paper; and FS designed the study, performed experiments, analyzed data, and wrote the paper.

Acknowledgements

Not applicable

References

1. Mitry D, Charteris DG, Fleck BW, Campbell H, Singh J. The epidemiology of rhegmatogenous retinal detachment: geographical variation and clinical associations. Br J Ophthalmol. 2010;94:678–84.
2. Mitry D, Awan MA, Borooah S, Siddiqui MAR, Brogan K, Fleck BW, et al. Surgical outcome and risk stratification for primary retinal detachment repair: results from the Scottish Retinal Detachment study. Br J Ophthalmol. 2012;96:730–4.
3. Ross WH. Visual recovery after macula-off retinal detachment. Eye (Lond). 2002;16:440–6.
4. Cook B, Lewis GP, Fisher SK, Adler R. Apoptotic photoreceptor degeneration in experimental retinal detachment. Invest Ophthalmol Vis Sci. 1995;36:990–6.
5. Murakami Y, Notomi S, Hisatomi T, Nakazawa T, Ishibashi T, Miller JW, et al. Photoreceptor cell death and rescue in retinal detachment and degenerations. Prog Retin Eye Res. 2013;37:114–40.
6. Dai Y, Wu Z, Sheng H, Zhang Z, Yu M, Zhang Q. Identification of inflammatory mediators in patients with rhegmatogenous retinal detachment associated with choroidal detachment. Mol Vis.

2015;21:417–27.

7. Kiang L, Ross BX, Yao J, Shanmugam S, Andrews CA, Hansen S, et al. Vitreous Cytokine Expression and a Murine Model Suggest a Key Role of Microglia in the Inflammatory Response to Retinal Detachment. Invest Ophthalmol Vis Sci. 2018;59:3767–78.
8. Pollreisz A, Sacu S, Eibenberger K, Funk M, Kivaranovic D, Zlabinger GJ, et al. Extent of Detached Retina and Lens Status Influence Intravitreal Protein Expression in Rhegmatogenous Retinal Detachment. Invest Ophthalmol Vis Sci. 2015;56:5493–502.
9. Takahashi S, Adachi K, Suzuki Y, Maeno A, Nakazawa M. Profiles of Inflammatory Cytokines in the Vitreous Fluid from Patients with Rhegmatogenous Retinal Detachment and Their Correlations with Clinical Features. Biomed Res Int. 2016;2016:4256183.
10. Kataoka K, Matsumoto H, Kaneko H, Notomi S, Takeuchi K, Sweigard JH, et al. Macrophage- and RIP3-dependent inflammasome activation exacerbates retinal detachment-induced photoreceptor cell death. Cell Death Dis. 2015;6:e1731.
11. Nakazawa T, Matsubara A, Noda K, Hisatomi T, She H, Skondra D, et al. Characterization of cytokine responses to retinal detachment in rats. Mol Vis. 2006;12:867–78.
12. Nakazawa T, Hisatomi T, Nakazawa C, Noda K, Maruyama K, She H, et al. Monocyte chemoattractant protein 1 mediates retinal detachment-induced photoreceptor apoptosis. Proc Natl Acad Sci USA. 2007;104:2425–30.
13. Nakazawa T, Kayama M, Ryu M, Kunikata H, Watanabe R, Yasuda M, et al. Tumor necrosis factor-alpha mediates photoreceptor death in a rodent model of retinal detachment. Invest Ophthalmol Vis Sci. 2011;52:1384–91.
14. Saleh M, Debellemanière G, Meillat M, Tumahai P, Bidaut Garnier M, Flores M, et al. Quantification of cone loss after surgery for retinal detachment involving the macula using adaptive optics. Br J Ophthalmol. 2014;98:1343–8.
15. Aït-Ali N, Fridlich R, Millet-Puel G, Clérin E, Delalande F, Jaillard C, et al. Rod-derived cone viability factor promotes cone survival by stimulating aerobic glycolysis. Cell. 2015;161:817–32.
16. Chertov AO, Holzhausen L, Kuok IT, Couron D, Parker E, Linton JD, et al. Roles of glucose in photoreceptor survival. J Biol Chem. 2011;286:34700–11.
17. Simpson IA, Dwyer D, Malide D, Moley KH, Travis A, Vannucci SJ. The facilitative glucose transporter GLUT3: 20 years of distinction. Am J Physiol Endocrinol Metab. 2008;295:E242–53.
18. Punzo C, Kornacker K, Cepko CL. Stimulation of the insulin/mTOR pathway delays cone death in a mouse model of retinitis pigmentosa. Nat Neurosci. 2009;12:44–52.
19. Venkatesh A, Ma S, Le YZ, Hall MN, Rüegg MA, Punzo C. Activated mTORC1 promotes long-term cone survival in retinitis pigmentosa mice. J Clin Invest. 2015;125:1446–58.
20. Ivanovic I, Anderson RE, Le YZ, Fliesler SJ, Sherry DM, Rajala RVS. Deletion of the p85alpha regulatory subunit of phosphoinositide 3-kinase in cone photoreceptor cells results in cone photoreceptor degeneration. Invest Ophthalmol Vis Sci. 2011;52:3775–83.

21. Rajala A, Dighe R, Agbaga M-P, Anderson RE, Rajala RVS. Insulin receptor signaling in cones. J Biol Chem. 2013;288:19503–15.
22. Kelly B, O'Neill LAJ. Metabolic reprogramming in macrophages and dendritic cells in innate immunity. Cell Res. 2015;25:771–84.
23. Shoelson SE, Lee J, Goldfine AB. Inflammation and insulin resistance. J Clin Invest. 2006;116:1793–801.
24. Machemer R, Aaberg TM, Freeman HM, Irvine AR, Lean JS, Michels RM. An updated classification of retinal detachment with proliferative vitreoretinopathy. Am J Ophthalmol. 1991;112:159–65.
25. Laskowski D, Sjunnesson Y, Gustafsson H, Humblot P, Andersson G, Båge R. Insulin concentrations used in in vitro embryo production systems: a pilot study on insulin stability with an emphasis on concentrations measured in vivo. Acta Vet Scand. 2016;58:66.
26. Pepper AR, Gall C, Mazzuca DM, Melling CWJ, White DJG. Diabetic rats and mice are resistant to porcine and human insulin: flawed experimental models for testing islet xenografts. Xenotransplantation. 2009;16:502–10.
27. Arroyo JG, Yang L, Bula D, Chen DF. Photoreceptor apoptosis in human retinal detachment. Am J Ophthalmol. 2005;139:605–10.
28. Hisatomi T, Sakamoto T, Murata T, Yamanaka I, Oshima Y, Hata Y, et al. Relocalization of Apoptosis-Inducing Factor in Photoreceptor Apoptosis Induced by Retinal Detachment in Vivo. Am J Pathol. 2001;158:1271–8.
29. Hisatomi T, Sakamoto T, Goto Y, Yamanaka I, Oshima Y, Hata Y, et al. Critical role of photoreceptor apoptosis in functional damage after retinal detachment. Curr Eye Res. 2002;24:161–72.
30. Guillonneau X, Eandi CM, Paques M, Sahel J-A, Sapieha P, Sennlaub F. On phagocytes and macular degeneration. Prog Retin Eye Res. 2017;61:98–128.
31. O'Koren EG, Mathew R, Saban DR. Fate mapping reveals that microglia and recruited monocyte-derived macrophages are definitively distinguishable by phenotype in the retina. Sci Rep. 2016;6:20636.
32. Calippe B, Augustin S, Beguier F, Charles-Messance H, Poupel L, Conart J-B, et al. Complement Factor H Inhibits CD47-Mediated Resolution of Inflammation. Immunity. 2017;46:261–72.
33. Ng TF, Turpie B, Masli S. Thrombospondin-1-mediated regulation of microglia activation after retinal injury. Invest Ophthalmol Vis Sci. 2009;50:5472–8.
34. Wang S, Sorenson CM, Sheibani N. Lack of thrombospondin 1 and exacerbation of choroidal neovascularization. Arch Ophthalmol. 2012;130:615–20.
35. Li Z, He L, Wilson K, Roberts D. Thrombospondin-1 inhibits TCR-mediated T lymphocyte early activation. J Immunol. 2001;166:2427–36.
36. Wang H, Qin J, Gong S, Feng B, Zhang Y, Tao J. Insulin-like growth factor-1 receptor-mediated inhibition of A-type K(+) current induces sensory neuronal hyperexcitability through the

phosphatidylinositol 3-kinase and extracellular signal-regulated kinase 1/2 pathways, independently of Akt. Endocrinology. 2014;155:168–79.

37. Chu Q, Moreland R, Yew NS, Foley J, Ziegler R, Scheule RK. Systemic Insulin-like growth factor-1 reverses hypoalgesia and improves mobility in a mouse model of diabetic peripheral neuropathy. Mol Ther. 2008;16:1400–8.
38. Kim JJ, Accili D. Signalling through IGF-I and insulin receptors: where is the specificity? Growth Horm IGF Res. 2002;12:84–90.
39. Siddle K, Ursø B, Niesler CA, Cope DL, Molina L, Surinya KH, et al. Specificity in ligand binding and intracellular signalling by insulin and insulin-like growth factor receptors. Biochem Soc Trans. 2001;29:513–25.
40. Leonardini A, Laviola L, Perrini S, Natalicchio A, Giorgino F. Cross-Talk between PPARgamma and Insulin Signaling and Modulation of Insulin Sensitivity. PPAR Res. 2009;2009:818945.
41. Matsui Y, Hirasawa Y, Sugiura T, Toyoshi T, Kyuki K, Ito M. Metformin reduces body weight gain and improves glucose intolerance in high-fat diet-fed C57BL/6J mice. Biol Pharm Bull. 2010;33:963–70.
42. Das LM, Rosenjack J, Au L, Galle PS, Hansen MB, Cathcart MK, et al. Hyper-inflammation and skin destruction mediated by rosiglitazone activation of macrophages in IL-6 deficiency. J Invest Dermatol. 2015;135:389–99.
43. Saisho Y. Metformin and Inflammation: Its Potential Beyond Glucose-lowering Effect. Endocr Metab Immune Disord Drug Targets. 2015;15:196–205.
44. Kunikata H, Yasuda M, Aizawa N, Tanaka Y, Abe T, Nakazawa T. Intraocular concentrations of cytokines and chemokines in rhegmatogenous retinal detachment and the effect of intravitreal triamcinolone acetonide. Am J Ophthalmol. 2013;155:1028–37.e1.
45. Matsumoto H, Kataoka K, Tsoka P, Connor KM, Miller JW, Vavvas DG. Strain difference in photoreceptor cell death after retinal detachment in mice. Invest Ophthalmol Vis Sci. 2014;55:4165–74.
46. Nakazawa T, Takeda M, Lewis GP, Cho K-S, Jiao J, Wilhelmsson U, et al. Attenuated glial reactions and photoreceptor degeneration after retinal detachment in mice deficient in glial fibrillary acidic protein and vimentin. Invest Ophthalmol Vis Sci. 2007;48:2760–8.
47. Wang X, Miller EB, Goswami M, Zhang P, Ronning KE, Karlen SJ, et al. Rapid monocyte infiltration following retinal detachment is dependent on non-canonical IL6 signaling through gp130. J Neuroinflammation. 2017;14:121.
48. Fu Y, Maianu L, Melbert BR, Garvey WT. Facilitative glucose transporter gene expression in human lymphocytes, monocytes, and macrophages: a role for GLUT isoforms 1, 3, and 5 in the immune response and foam cell formation. Blood Cells Mol Dis. 2004;32:182–90.
49. Costa Rosa LF, Safi DA, Cury Y, Curi R. The effect of insulin on macrophage metabolism and function. Cell Biochem Funct. 1996;14:33–42.
50. Liu X, Mameza MG, Lee YS, Eseonu CI, Yu C-R, Kang Derwent JJ, et al. Suppressors of Cytokine-Signaling Proteins Induce Insulin Resistance in the Retina and Promote Survival of Retinal Cells.

Diabetes. 2008;57:1651–8.

51. Eandi CM, Charles Messance H, Augustin S, Dominguez E, Lavalette S, Forster V, et al. Subretinal mononuclear phagocytes induce cone segment loss via IL-1β. Elife. 2016;5.

Figures

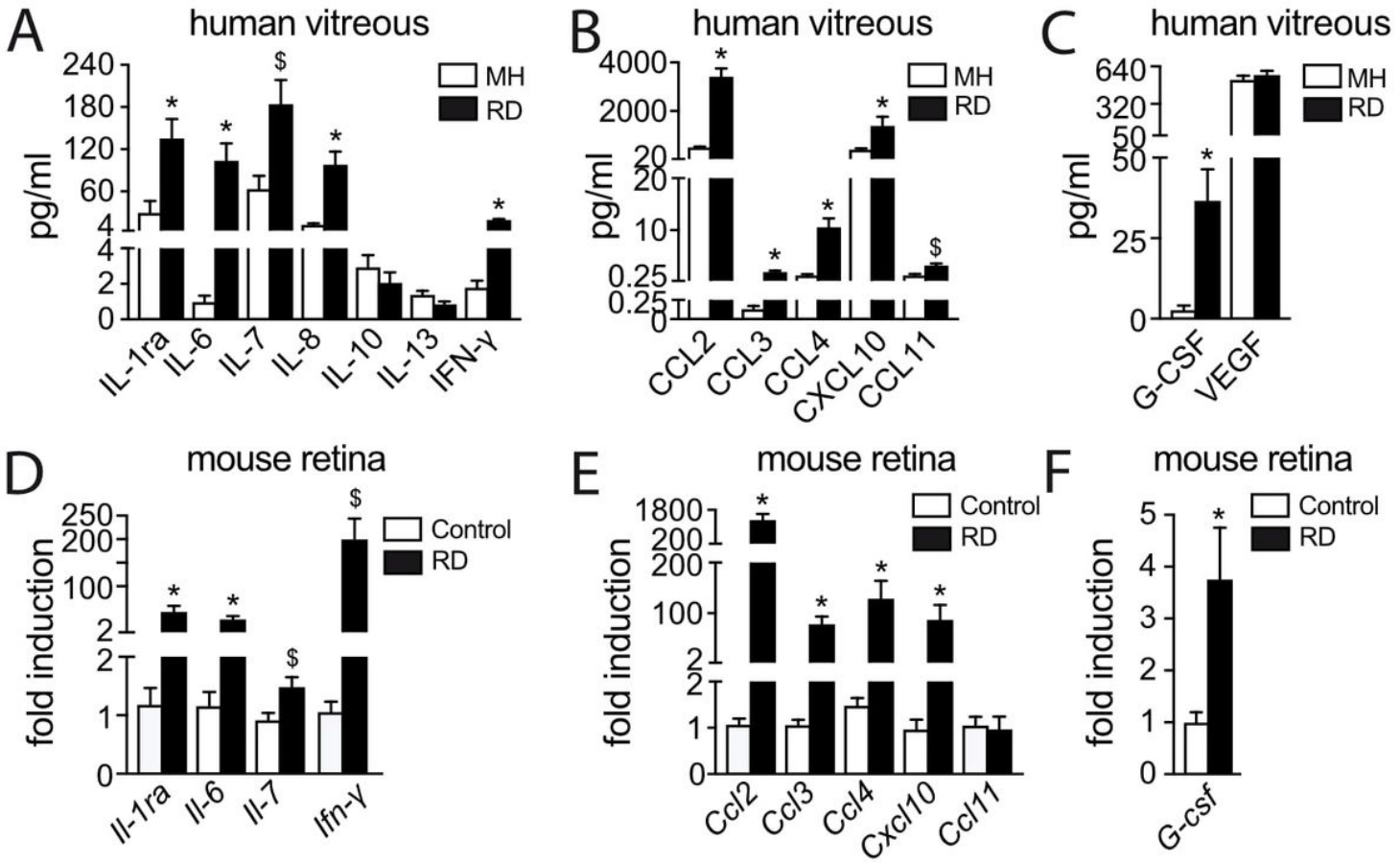

Figure 1

RD causes a marked inflammatory response with increased cytokine and chemokine expression in both human and experimental models (A-C) Vitreous concentrations of (A) cytokines, (B) chemokines and (C) growth factors from MH and RD groups of patients (34 MH and 41 RD samples; A: t-test or Mann-Whitney U test *p < 0.0001 and $p = 0.009 versus control; B: t-test or Mann-Whitney U test *p < 0.0001 and $p = 0.002 versus control; C: t-test *p = 0.002 versus control). (D-F) Relative expression of (D) cytokine, (E) chemokine and (F) growth factor mRNAs normalized with S26 expression quantified by RT-qPCR in mouse retina without RD and 4 days after RD (n = 6-8/group; Mann-Whitney U test *p < 0.01 and $p = 0.03 versus control) RD: retinal detachment; MH: macular hole. All values are reported as mean ± SEM.

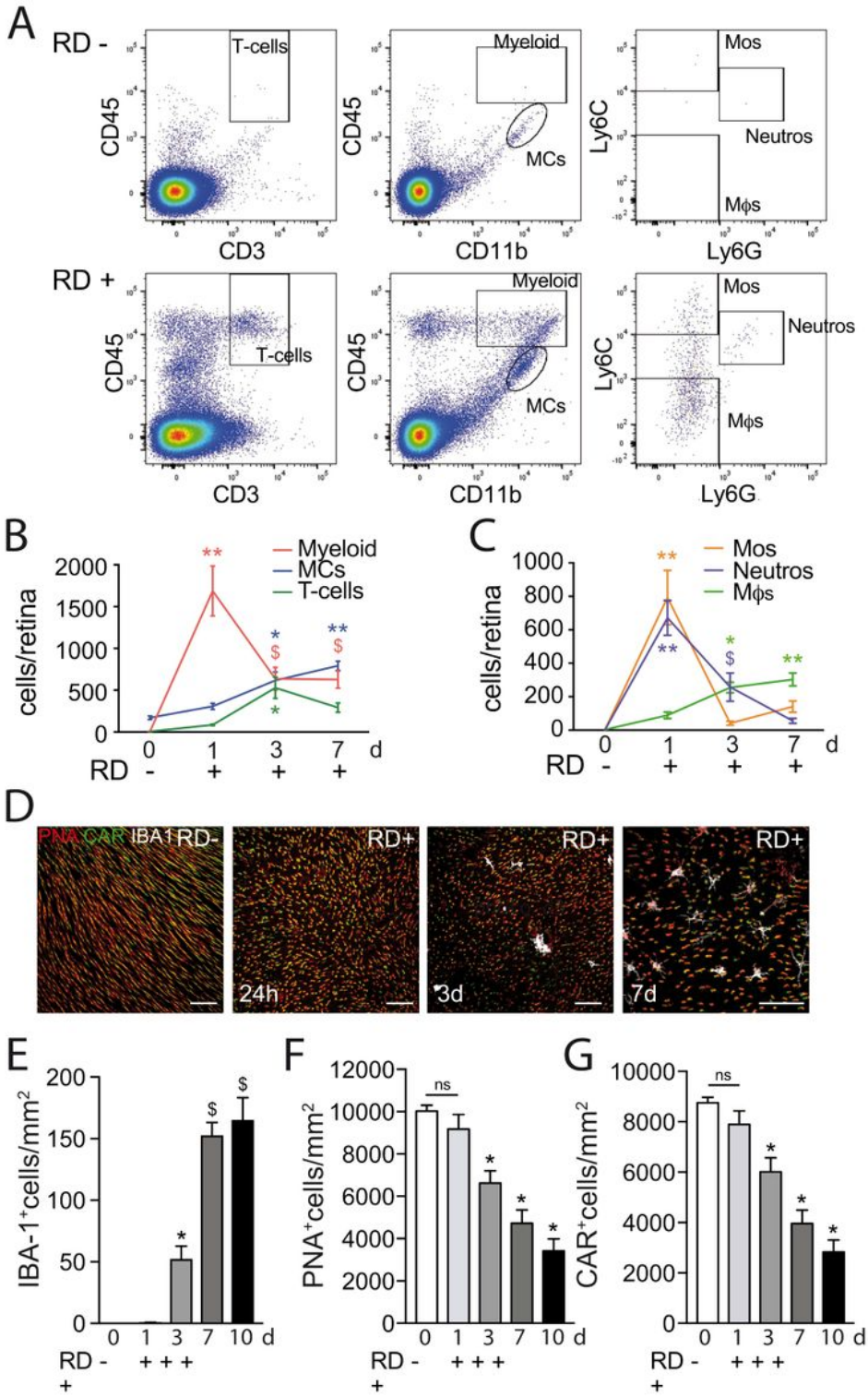

Figure 2

RD-associated leukocyte infiltration is associated with cone loss (A) Representative cytometry plots of mouse retina without RD (upper panels) or 7 days after RD (lower panels). CD45+CD3+ cells define T-cells and CD45+CD11b+ cells define microglia and myeloid cells with CD45lowCD11b+ representing microglia and CD45highCD11b+ representing infiltrating myeloid cells. CD45highCD11b+ were further defined with Ly6C and Ly6G with Ly6ChighLy6C- cells representing monocytes, Ly6ClowLy6C- representing

macrophages and Ly6G+ representing neutrophils. (B-C) Flow cytometry quantification of (B) T-cells, MCs and infiltrating myeloid cells and (C) Mos, Mφs and neutrophils in mouse retina without RD and 24 hours, 3 days and 7 days after RD (n = 8-16/group; B: one-way Anova *p < 0.006, **p <0 .0001 and $p < 0.05 versus the control group; C: one-way Anova *p = 0.0016, **p <0 .0001 and $p = 0.0384 versus the control group) (D) Representative images of peanut agglutinine- (PNA, red), cone arrestin- (CAR, green) and ionized calcium-binding adaptater molecule 1- (IBA-1, white) stained retinal flatmounts of C57BL6/J mice without RD, 24h hours, 3 days and 7 days after RD. (E-G) Quantification of (E) subretinal IBA-1+ cells, (F) PNA+ cones and (G) CAR+ cones in retinal flatmounts of C57BL6/J mice without RD and one day, 3 days, 7 days and 10 days after RD (n = 6-12/group; E: one-way Anova *p = 0.0153 and $p < 0.0001 versus the control group; F: one-way Anova *p < 0.0001 versus the control group; G: one-way Anova *p < 0.0001 versus the control group). RD: retinal detachment; Myeloid: myeloid cells; Mos: monocytes; MCs microglial cells; Mφs: macrophages; Neutros: neutrophils; PNA: peanut agglutinine; CAR: cone arrestin; IBA-1: ionized calcium-binding adaptater molecule 1. Scale bar D = 50µm. All values are reported as mean ± SEM.

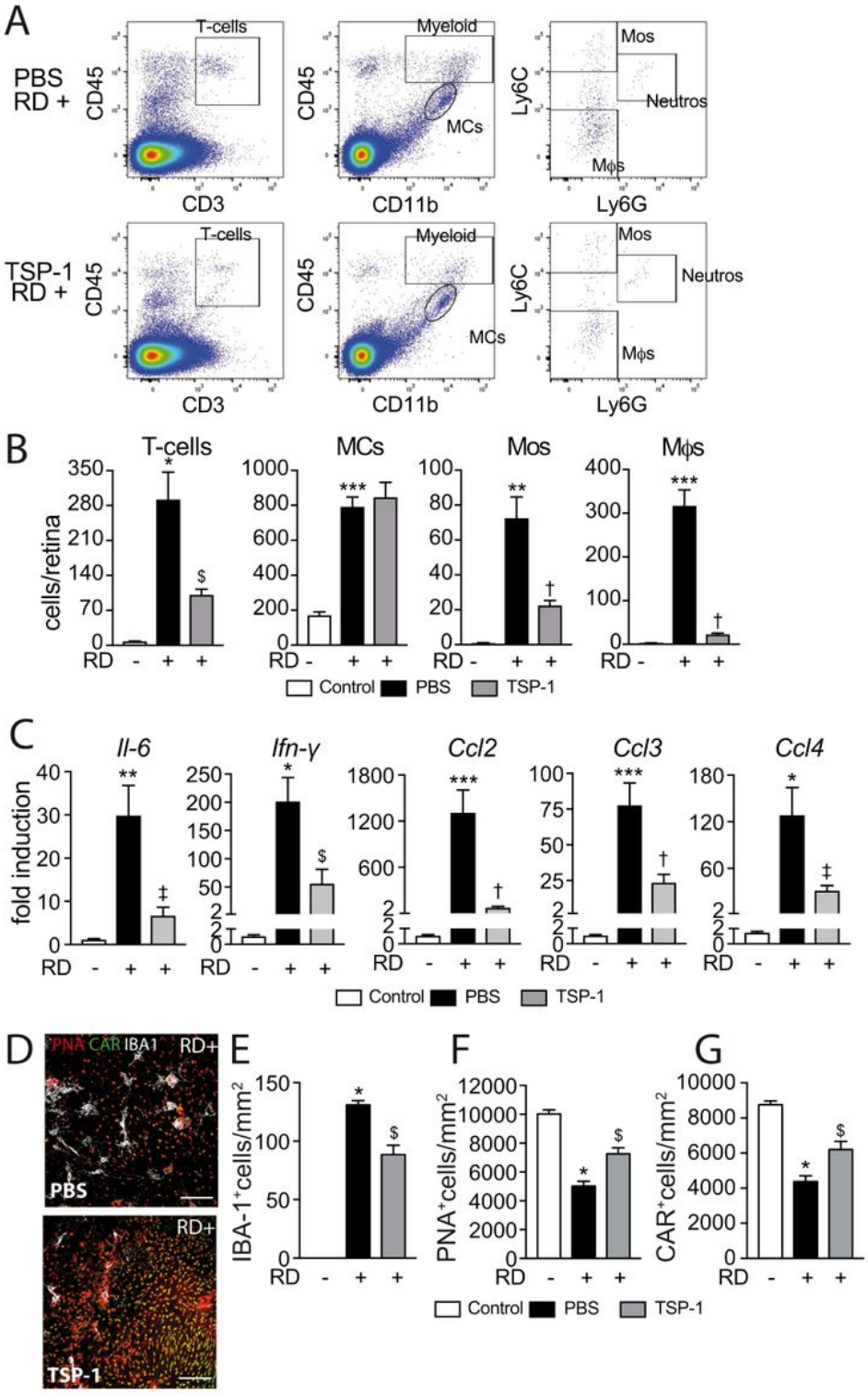

Figure 3

TSP-1 inhibits RD-induced leukocyte infiltration and prevents cone loss (A) Representative cytometry plots of mouse retina 7 days after RD without (upper panels) or with subretinal injection of TSP-1 (lower pannels). CD45+CD3+ cells define T-cells and CD45+CD11b+ cells define microglia and myeloid cells with CD45lowCD11b+ representing microglia and CD45highCD11b+ representing infiltrating myeloid cells. CD45highCD11b+ were further defined with Ly6C and Ly6G with Ly6ChighLy6C- cells representing

monocytes, Ly6ClowLy6C- representing macrophages and Ly6G+ representing neutrophils. (B) Flow cytometry quantification of T-cells, MCs, Mos and Mφs in mouse retina without RD and 7 days after RD without or with subretinal injection of TSP-1 (n = 8-24/group; one-way Anova/Bonferroni test *p = 0.0018, **p = 0.0003 and ***p < 0.0001 versus the control group, $p = 0.0032 and †p < 0.0005 versus the PBS group) (C) Quantitative RT-PCR of Il-6, Ifn-γ, Ccl2, Ccl3 and Ccl4 mRNAs normalized to S26 mRNA in mouse retina without RD and 4 days after RD with or without subretinal injection of TSP-1 (n = 6-8/group; one-way Anova/Bonferroni test *p < 0.003, **p < 0.001 and ***p < 0.0001 versus the control group, $p < 0.01, ‡p < 0.007 and †p < 0.0005 versus the PBS group) (D) Representative images of peanut agglutinine- (PNA, red), cone arrestin- (CAR, green) and ionized calcium-binding adaptater molecule 1- (IBA-1, white) stained retinal flatmounts of C57BL6/J mice 7 days after RD without or with subretinal injection of TSP-1. (E-G) Quantification of (E) subretinal IBA-1+ cells, (F) PNA+ cones and (G) CAR+ cones in retinal flatmounts of C57BL6/J mice without RD and 7 days after RD without or with subretinal injection of TSP-1 (n = 6-12/group; E: one-way Anova/Bonferroni test *p < 0.0001 versus the control group, $p = 0.0002 versus the PBS group; F: one-way Anova/Bonferroni test *p < 0.0001 versus the control group, $p = 0.0470 versus the PBS group; G: one-way Anova/Bonferroni test *p < 0.0001 versus the control group, $p = 0.0448 versus the PBS group). RD: retinal detachment; PBS: phosphate buffered saline; TSP-1: thrombospondin-1; Myeloid: myeloid cells; Mos: monocytes; MCs microglial cells; Mφs: macrophages; Neutros: neutrophils; PNA: peanut agglutinine; CAR: cone arrestin; IBA-1: ionized calcium-binding adaptater molecule 1. Scale bar D = 50µm. All values are reported as mean ± SEM.

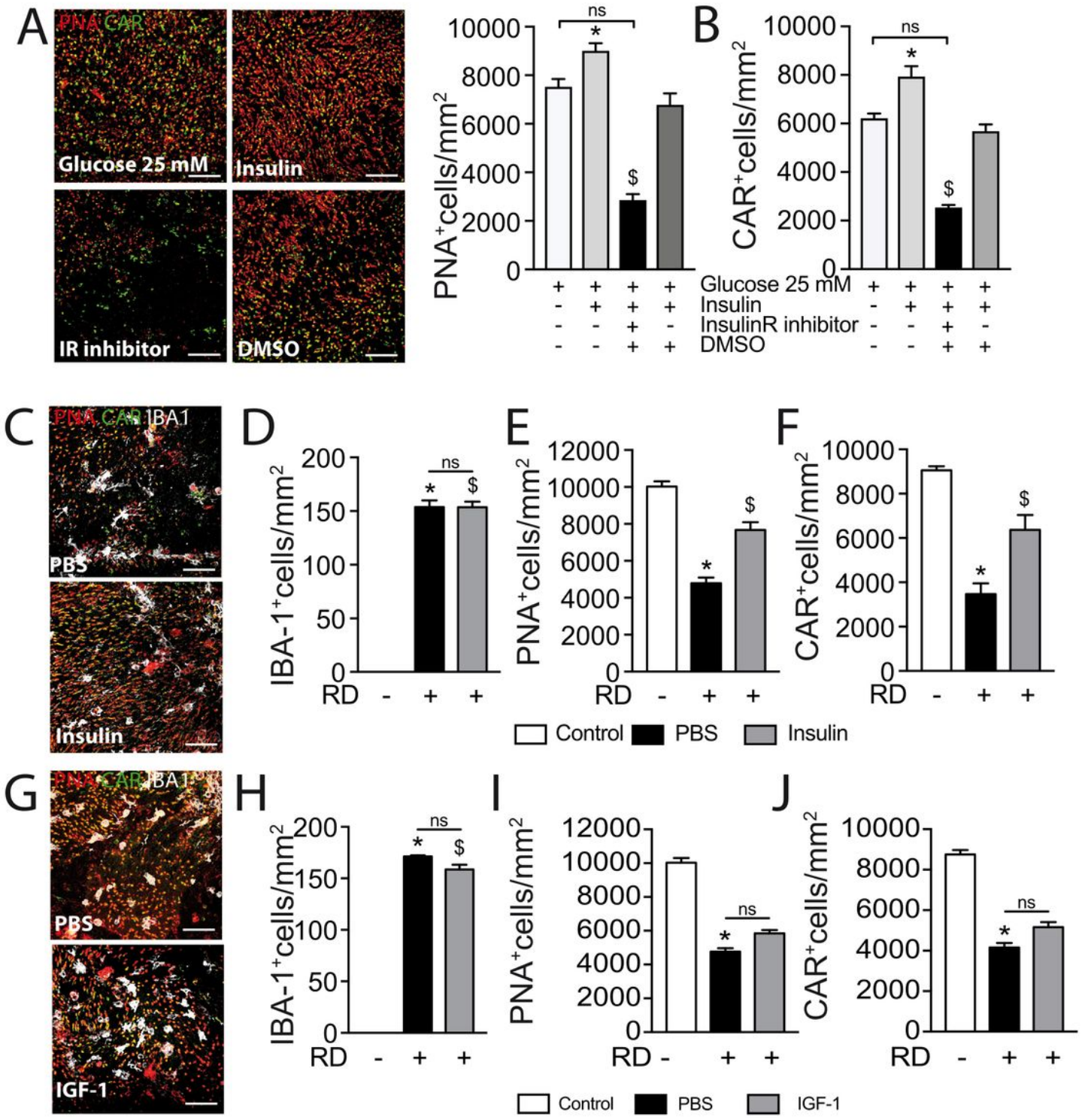

Figure 4

Insulin is essential for cone survival in vitro and delays RD-induced cone loss in vivo (A and B) Representative images of peanut agglutinine- (PNA, red) and cone arrestin- (CAR, green) stained retinal explants and quantification of (A) PNA+ cones and (B) CAR+ cones after 5 days of culture in high glucose DMEM (25mM) with or without human insulin and/or insulin receptor inhibitor (HNMPA) or its vehicle (n = 5/group; B: one-way Anova *p = 0.0358 and $p < 0.0001 versus the high glucose culture; C: one-way

Anova *p = 0.0012 and $p < 0.0001 versus the high glucose culture). (C) Representative images of peanut agglutinine- (PNA, red), cone arrestin- (CAR, green) and ionized calcium-binding adaptater molecule 1- (IBA-1, white) stained retinal flatmounts of C57BL6/J mice 7 days after RD without or with subretinal injection of insulin. (D-F) Quantification of (D) subretinal IBA-1+ cells, (E) PNA+ cones and (F) CAR+ cones in retinal flatmounts of C57BL6/J mice without RD and 7 days after RD with or without subretinal injection of insulin (n = 6-12/group; E: one-way Anova *p < 0.0001 and $p < 0.0001 versus the control group; F: one-way Anova/Bonferroni test *p < 0.0001 versus the control group, $p = 0.0020 versus the PBS group; G: one-way Anova/Bonferroni test *p < 0.0001 versus the control group, $p = 0.0002 versus the PBS group) (G) Representative images of peanut agglutinine- (PNA, red), cone arrestin- (CAR, green) and ionized calcium-binding adaptater molecule 1- (IBA-1, white) stained retinal flatmounts of C57BL6/J mice 7 days after RD without or with subretinal injection of IGF-1. (H-J) Quantification of (H) subretinal IBA-1+ cells, (I) PNA+ cones and (J) CAR+ cones in retinal flatmounts of C57BL6/J mice without RD and 7 days after RD with or without subretinal injection of IGF-1 (n = 6-12/group; G: one-way Anova *p < 0.0001, $p < 0.0001 versus the control group; H: one-way Anova *p < 0.0001 versus the control group; I: one-way Anova *p < 0.0001 versus the control group). PNA: peanut agglutinine; CAR: cone arrestin; IR: insulin receptor; DMSO: dimethyl sulfoxide; IBA-1: ionized calcium-binding adaptater molecule 1; PBS: phosphate buffered saline; RD: retinal detachment; IGF-1: insulin-like gro wth factor; DMEM: Dulbecco's modified Eagle's medium; HNMPA: hydroxy-2-naphthalenylmethylphosphonic acid Scale bar A, C and G = 50µm. All values are reported as mean ± SEM.

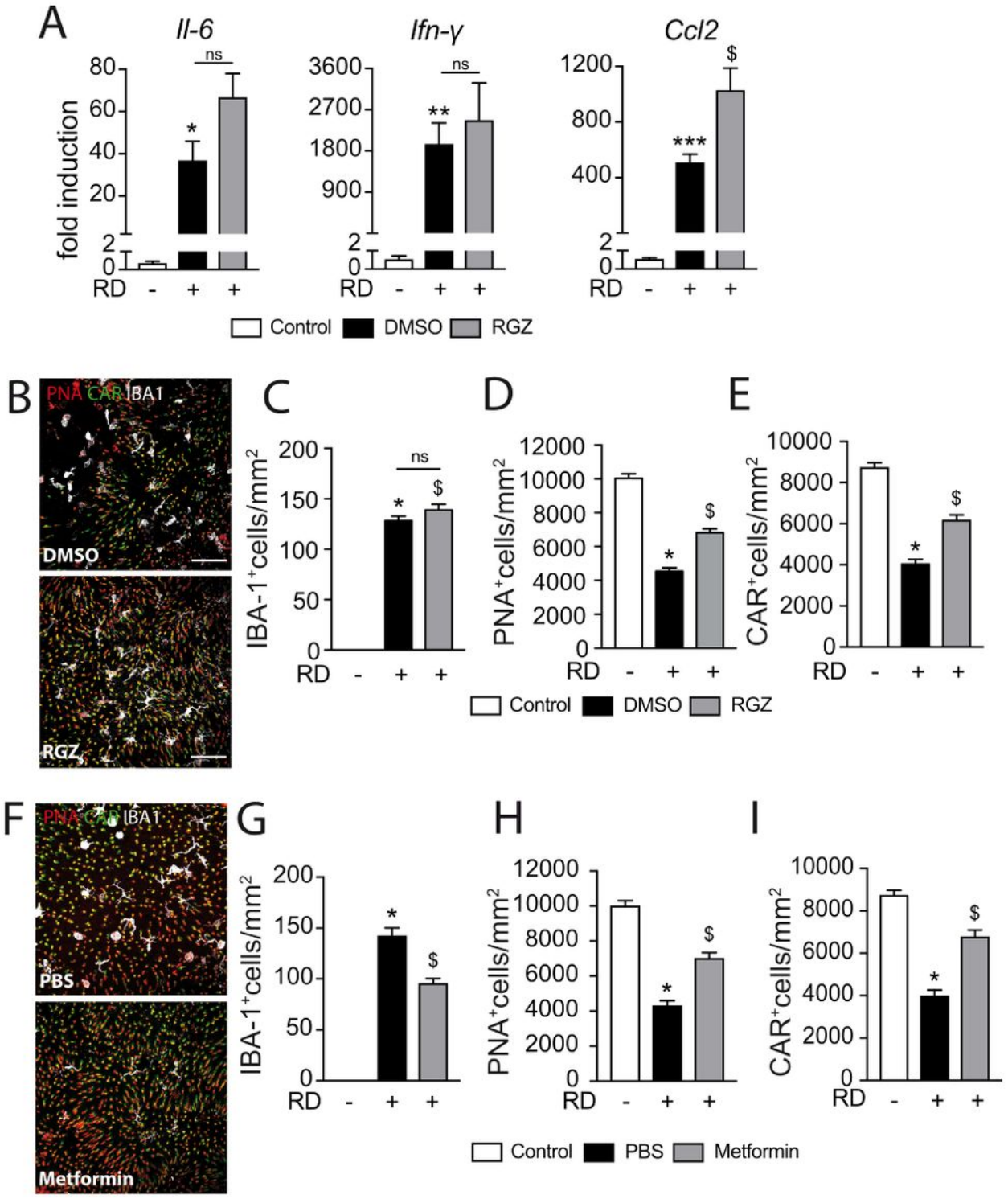

Figure 5

The insulin sensitizer rosiglitazone prevents RD-induced cone loss (A) Quantitative RT-PCR of Ccl2, Il-6 and Ifn-γ mRNAs normalized to S26 mRNA in mouse retina without RD and 4 days after RD and treatment with rosiglitazone or its vehicle (n = 6-10/group; one-way Anova/Bonferroni test *p = 0.0494, **p = 0.0326 and ***p = 0.0036 versus the control group, $p = 0.0028 versus the DMSO group). (B) Representative images of peanut agglutinine- (PNA, red), cone arrestin- (CAR, green) and ionized calcium-

binding adaptater molecule 1- (IBA-1, white) stained retinal flatmounts of C57BL6/J mice 7 days after RD and treatment with rosiglitazone or its vehicle (DMSO) . (C-E) Quantification of (C) of subretinal IBA-1+ cells, (D) PNA+ cones and (E) CAR+ cones in retinal flatmounts of C57BL6/J mice without RD and 7 days after RD and treatment with rosiglitazone or its vehicle (n = 6-12/group; C: one-way Anova *p < 0.0001 and $p < 0.0001 versus the control group D: one-way Anova/Bonferroni test *p < 0.0001 versus the control group, $p = 0.0018 versus the DMSO group; E: one-way Anova/Bonferroni test *p < 0.0001 versus the control group, $p = 0.0031 versus the DMSO group). (F) Representative images of peanut agglutinine- (PNA, red), cone arrestin- (CAR, green) and ionized calcium-binding adaptater molecule 1- (IBA-1, white) stained retinal flatmounts of C57BL6/J mice 7 days after RD without or with subretinal injection of metformin. (G-I) Quantification of (G) subretinal IBA-1+ cells, (H) PNA+ cones and (I) CAR+ cones in retinal flatmounts of C57BL6/J mice without RD and 7 days after RD without or with subretinal injection of metformin (n = 6-12/group; G: one-way Anova *p < 0.0001 versus the control group, $p < 0.0001 versus the PBS group; H: one-way Anova *p < 0.0001 versus the control group, $p = 0.0056 versus the PBS group; I: one-way Anova *p < 0.0001 versus the control group, $p = 0.0004 versus the PBS group). RD: retinal detachment; DMSO: dimethyl sulfoxyde; RGZ: rosiglitazone; PNA: peanut agglutinine; CAR : cone arrestin; IBA-1: ionized calcium-binding adaptater molecule 1. Scale bar A, B and F = 50µm. All values are reported as mean ± SEM.